Astron. Astrophys. 340, 419–430 (1998)

ASTRONOMY AND ASTROPHYSICS

A simple convection model for selfgravitating fluid dynamics

Time-dependent convective energy transfer in protostars and nonlinear stellar pulsations

G. Wuchterl and M.U. Feuchtinger

Institut für Astronomie der Universität Wien, Türkenschanzstrasse 17, A-1180 Wien, Austria

Received 15 July 1998 / Accepted 2 October 1998

Abstract. We describe a relatively simple time-dependent convection model that can be coupled to the equations of radiation hydrodynamics. We show that it behaves in a physically plausible way in protostellar collapse flows and is quantitatively correct for nonlinear RR-Lyrae pulsations and the Sun. Together with the equations of radiation hydrodynamics the model closely approximates the classical stellar structure equations with mixing length convection for a set of standard assumptions.

Key words: convection – hydrodynamics – stars: formation – stars: oscillations

1. Introduction

Radiation and self-gravity dominate many astrophysical situations. However, the relative inefficiency of heat conduction and radiative transfer in stars and giant planets rapidly produce convectively unstable situations. Often convection plays the role of the dominating heat transfer process. When the evolution of the flow, say in a star, becomes so rapid that the evolutionary time scale is comparable to the rise time of bouyancy driven convective eddies over a distance where the flow quantities change considerably, the mesoscopic dynamics of the eddies couples and interacts with the macroscopic dynamics of the overall flow. Hence, a model of those effects, a model for time-dependent turbulent convection, is needed to calculate the flow correctly.

The classical example for such situations are stellar pulsations where the dynamical time-scale

$$\tau_{\rm dyn} \approx P_0 \approx \tau_{\rm ff} \approx 2494\sqrt{\frac{\bar{\varrho_\odot}}{\varrho}}\,[\rm s] \quad (1)$$

becomes comparable with the inverse of the Brunt-Väisälä frequency, N (Kippenhahn & Weigert 1990)

$$\tau_{\rm bouy} = \frac{1}{N} = \frac{H_p}{c_{\rm s}}\sqrt{\frac{\Gamma_1}{\delta(\nabla_s - \nabla)}} \approx 23.08\frac{[g_\odot]}{g}\sqrt{\frac{T}{T_\odot}}\,[\rm s] \quad (2)$$

Send offprint requests to: M.U. Feuchtinger
(fm@amok.astro.univie.ac.at)

$$N^2 = -\frac{g\delta}{H_p}(\nabla_s - \nabla) = \frac{g\delta}{c_p}\frac{\partial s}{\partial r}. \quad (3)$$

Note that the sign for N^2 has been reversed to obtain a real timescale for convective instability.

Usually stellar pulsations are driven by the so-called κ- and γ- mechanisms acting in the ionisation zones of hydrogen and helium which are located in the outer layers of the stellar envelope. As long as the energy is carried by radiation in these zones the interaction between the radiation field and the strongly temperature dependent opacity of the stellar plasma leads to the well-known vibrational instability growing up to finite amplitude oscillations. On the other hand convective instability which physically is closely related to the vibrational instability, occurs right in those ionisation regions responsible for the pulsational driving. Consequently the driving mechanism diminishes if more and more of the flux is carried by convection leading e.g. to the red edge of the classical instability strip. In that way time-dependent turbulent convection plays a fundamental role for the modal stability and for the limit cycle characteristics of pulsating stars (e.g. Bono & Stellingwerf 1994).

Another important example is the initial creation of convective regions in star- and giant planet formation where convection arises typically in stable radiative zones when they are rapidly heated by gravitational contraction or collapse phenomena. A description of the time evolution from zero to finite eddy-velocities is needed in those cases. A somewhat opposite situation, that typically occurs in the bounces of protostellar cores is the damping of convection due to rapid expansion of the flow. Here a physically meaningful description has to show damping of convection on a finite time scale.

All astrophysical scenarios mentioned so far have in common, that convective instability occurs in flows that are non-hydrostatic, requiring the solution of the equations of motion to determine their temporal evolution. But even in hydrostatic situations changes may occur faster than convection can evolve to a steady state. Examples are again rapid quasi-hydrostatic contraction in star- and giant planet formation where convection is “switched on” in entirely radiative gas-spheres. But there is no reason why quasi-hydrostatic stellar expansion in late stellar evolution should always be slower than the respective convective relaxation time (see Deupree 1984, 1986 for core He flashes,

Starrfield & Cox, 1989 for white dwarf pulsations and Glasner & Livne, 1995 for Novae). A condition that has to be satisfied in order to use static convection models like the mixing length theory or the model by Canuto & Mazzitelli (1991).

In this paper we describe a model that is capable to account for the mostly qualitative requirements of star- and giant planet formation caculations and at the same time satisfy the quantitative demands of stellar pulsation calculations. We focus on two primary time-dependent effects in convective energy transfer:

1. The energy exchange between gas and radiation on the one hand and convective eddies on the other. This is an intrinsically time-dependent effect, where convection plays the role of an additional degree of freedom, with an extra energy equation in the flow dynamics.
2. Non-instantaneous values for convective energy-fluxes and convective velocities.

In Sect. 2 we discuss the demands on a time-dependent model of turbulent convection as seen from the relatively unusual but nevertheless fundamental view of nonlinear astrophysical modelling. Starting with the investigation of giant planet formation (Wuchterl 1995b) this discussion leads to the choice of the one-equation convection model developed in Kuhfuß (1987) which offers several advantages as already presented in Wuchterl (1995a). A brief summary of this model which subsequently we call the *original Kuhfuß model* is given in Sect. 3. From test calculation involving the three different astrophysical scenarios of *star formation*, *stellar pulsations* and *giant planet formation* it turns out that the original version of this model does not satisfy the demands of being physically plausible and compatible with observational facts. Henceforth in Sect. 4 we increase the complexity of the original model, ending up with a modified version of the Kuhfuß model. A complete summary of this model is given in Sect. 5, Sect. 6 and 7 discuss the local static limit and free parameters and in Sect. 8 we compare the hydrostatic structure of a solar-like envelope calculated by using the different versions of the Kuhfuß model with a recent solar standard model. Sect. 9 closes the paper.

2. General remarks on turbulent convection models

One widely used way of understanding the physical processes responsible for what we observe in astrophysical objects is to develop and investigate realistic models which are capable of reproducing the observed data. In general the requirement of realistic models is inseparable connected with considering complex nonlinear and time-dependent interactions between several components like matter, radiation field, turbulent convection, magnetic fields etc. Consequently an appropriate model of time-dependent turbulent convection is subject to several demands which we summarise briefly in the following points

– In particular we concentrate our view on stars and stellar-like objects as protostars and giant planets, which in general have to be described within the framework of radiation hydrodynamics. In that sense our first demand on a model of time-dependent turbulent convection is, that it can be included into and solved together with the corresponding system of nonlinear PDE's describing the spatial structure and temporal evolution of radiating flows.
– A solution of such complex systems with realistic constitutive relations, initial- and boundary conditions usually involves sophisticated numerical methods and from this point of view suitable convection models have to be mathematically well behaved and free of singularities.
– Due to the lack of a self-consistent theory of turbulence each convection model is based on different assumptions and various levels of approximations. Consequently several free parameters have to be adjusted in order to fit the observational constraints. Therefore we focus on convection models with relatively few free parameters obeying physically meaningful definitions. Moreover we want to be able to follow the consequences of assumptions and approximations in the derivation of the model.
– In hydrostatic stellar structure and evolution calculations the generally accepted mixing length theory plays a fundamental role in describing static turbulent convection. In the case of pure radiative configurations the corresponding stellar structure equations can be obtained as the hydrostatic limit of the equations of radiation hydrodynamics. In that sense a desired property of the extended system of convective radiation hydrodynamics is the reduction to the mixing-length stellar structure equations in case of vanishing time-derivatives and gas velocities.

Lead by the above demands that became apparent in models of giant planet formation (cf. Wuchterl 1995b), Wuchterl (1995a) chose the simplest version of the turbulent convection model of Kuhfuß (1987). All necessary reformulations and the numerical method of solution on self-adaptive grids are given in Wuchterl (1995a). For a comparative discussion of time-dependent convection models see the review by Baker (1987).

3. The original model of Kuhfuß (1987)

In the following section we give a brief overview of the original one-equation model of time-dependent turbulent convection developed in Kuhfuß (1986). For further details we refer to the PHD-thesis of Kuhfuß (1987) and to the original paper. We assume spherical symmetry throughout the article. The fundamental physical quantity describing the convective field is the specific turbulent kinetic energy density $\bar{\omega}$ (for a comprehensive list of symbols we refer to Table A1 in the appendix). The temporal evolution of $\bar{\omega}$ is governed by the turbulent kinetic energy equation reading

$$\frac{d\bar{\omega}}{dt} = S_{\bar{\omega}} - \tilde{S}_{\bar{\omega}} - \frac{1}{\rho}\nabla\cdot j_t - \frac{P_t}{\rho}\nabla\cdot u + \frac{1}{\rho}E_Q\,. \tag{4}$$

The generation of turbulent kinetic energy through bouyancy forces $S_{\bar{\omega}}$ is given by

$$S_{\bar{\omega}} = \frac{T}{P}\frac{\partial P}{\partial r}\nabla_s\,\Pi \tag{5}$$

The basic quantity in this relation is the correlation Π between entropy and velocity fluctuations. One central assumption in Kuhfuß (1986) is to model this correlation by a diffusion approximation inferring the specific entropy gradient $\partial s/\partial r$ yielding

$$\Pi = -\alpha_s \, \Lambda \, \bar{\omega}^{1/2} \, \frac{\partial s}{\partial r} \tag{6}$$

where α_s denotes a free parameter and Λ the typical convective length scale (mixing length, cf. Sect. 4.1). Note that

$$\frac{\partial s}{\partial r} = -\frac{c_P}{H_\mathrm{p}} \left(\nabla - \nabla_s \right) \tag{7}$$

with actual and isentropic temperature gradient defined as

$$\nabla = \frac{P}{T} \frac{\partial T}{\partial P} \qquad \text{and} \qquad \nabla_s = \frac{P}{T} \left(\frac{\partial T}{\partial P} \right)_s \tag{8}$$

relates the turbulent driving function to the well known Schwarzschild criterion. The correlation Π also enters the convective enthalpy flux (energy transport through convection) given by

$$j_w = \rho \, T \, \Pi \tag{9}$$

which serves as an additional divergence term in the gas energy equation.

Dissipation of turbulent kinetic energy $\tilde{S}_{\bar{\omega}}$ through conversion of the turbulent motions into thermal energy is modelled by dimensional arguments leading to

$$\tilde{S}_{\bar{\omega}} = c_D \, \frac{\bar{\omega}^{3/2}}{\Lambda} \tag{10}$$

where c_D denotes a free parameter.

The turbulent kinetic energy flux approximated by diffusion of $\bar{\omega}$ is given by

$$j_t = \alpha_t \rho \, \Lambda \, \bar{\omega}^{1/2} \, \frac{\partial \bar{\omega}}{\partial r} \tag{11}$$

and is responsible for the nonlocal character of the convection model (overshooting). The overshooting distance is adjusted by means of the free parameter α_t.

The dissipation through turbulent Reynolds stresses is treated analogous to the molecular viscosity. The resulting Reynolds tensor is divided into a trace part yielding the turbulent pressure

$$P_t = \frac{2}{3} \rho \, \bar{\omega} \tag{12}$$

and a trace-free part leading to the turbulent viscosity. The corresponding viscous energy dissipation can be written as

$$E_Q = \frac{4}{3} \, \mu_Q \left\{ \frac{\partial u}{\partial r} - \frac{u}{r} \right\}^2 \tag{13}$$

where the kinetic turbulent viscosity

$$\mu_Q = \alpha_\mu \rho \, \Lambda \, \bar{\omega}^{1/2} \tag{14}$$

contains a free parameter α_μ. An additional term accounting for the momentum transfer through viscous forces reads

$$U_Q = \frac{1}{r^3} \frac{\partial}{\partial r} \left\{ \frac{4}{3} \mu_Q \, r^3 \left[\frac{\partial u}{\partial r} - \frac{u}{r} \right] \right\} \tag{15}$$

and has to be included to the right hand side of the equation of motion.

4. Modifications

The basic strategy of including a time-dependent convection model into our radiation hydrodynamical model was to start with the simplest version and apply the resulting code to different problems in stellar astrophysics. From those test computations several difficulties turned out and consequently we were forced to include several modifications which are discussed in the following sections.

4.1. Turbulent length scale Λ (mixing length)

Originally the convective length scale Λ is assumed to be proportional to the local pressure scale height $H_\mathrm{p} = -\partial r / \partial \ln P$. While this is a usefull parameterisation in hydrostatic and quasi-hydrostatic stellar structure and evolution applications, in hydrodynamical flows this formulation becomes singular whenever $\partial P/\partial r$ vanishes (e.g. in the rarefaction region behind an upward moving mass shell). To avoid this singularity we write the mixing length in terms of the the hydrostatic pressure scale height

$$H_P^\mathrm{stat} = -\left(\frac{\partial r}{\partial \ln P} \right)_\mathrm{hydrostatic} = \frac{r^2 \, P}{G m_r \, \rho} \tag{16}$$

meaning the pressure scale height of a hydrostatic equilibrium corresponding to the values of pressure P and density ρ in the actual flow. Under conditions of weak gravity encountered e.g. in the extended envelopes of protostars and proto-giant planets further complications arise as $H_P^\mathrm{stat}/r > 1$. We assume the local radius r to be an appropriate lengthscale for meassuring the largest scale turbulent motions and adopt a harmonic mean

$$\frac{1}{\Lambda} = \frac{1}{\alpha_\mathrm{ML} \, H_P^\mathrm{stat}} + \frac{1}{\beta_r r} \tag{17}$$

as a parameterisation for the mixing length that is physically reasonable under all conditions and reduces to the standard MLT prescription under 'normal' hydrostatic conditions with $H_P^\mathrm{stat}/r < 1$. The standard mixing length parameter is denoted by α_ML and the free parameter β_r is used to limit Λ under weak gravity conditions.

4.2. Radiative cooling of convective elements

In the original model of Kuhfuß (1986) developed for stellar evolution calculations the energy exchange between convective elements and their surroundings through radiation is not taken into account. This approximation is valid as long as convection is restricted to optically very thick regions encountered e.g. in

the deep interior of stars. However, having in mind typical astrophysical applications like giant planet formation, protostellar flows or nonlinear stellar pulsations and last but not least for the sun, we recall that convection zones may extend to moderate optical depths (e.g. photospheric convection) and consequently in general radiative losses cannot be neglected. Therefore we propose an additional term on the right-hand-side of Eq. 4 approximating the radiative energy exchange $D_{\rm rad}$ by a relaxation ansatz

$$D_{\rm rad} = \frac{\bar{\omega}}{\tau_{\rm rad}} \tag{18}$$

analogous to the mixing length theory (MLT) and the 3-equation model for turbulent convection described in Kuhfuß (1987), respectively. The typical cooling time scale of convective elements

$$\tau_{\rm rad} = \frac{c_p\,\kappa\,\rho^2\,\Lambda^2}{4\sigma\,T^3\,\gamma_{\rm R}^2} \tag{19}$$

is evaluated by assuming radiation diffusion between the convective bubble and its surrounding medium, and contains a free parameter $\gamma_{\rm R}$. In Sect. 6 we show that the value of $\gamma_{\rm R}$ can be choosen in order to approximate the MLT as the static local limit of Eq. 4.

4.3. Turbulent enthalpy flux

Calculations of the protostellar collapse point to a key problem of the simple original model, the violation of the diffusion approximation for the turbulent enthalpy flux, that essentially comes from a violation of modelling the correlation Π (Eq. 6) between entropy and velocity fluctuations by a diffusion ansatz. To explain the situation we derive a typical diffusion velocity u_D for the enthalpy w carried by convection in the following way. Bearing in mind that j_w is an enthalpy flux we can write it as $j_w = \rho\, w\, u_D$, noting that the specific enthalpy is given by $w = e + P/\rho$. Consequently for u_D follows

$$u_D = \frac{T}{w}\,\Pi\,. \tag{20}$$

On the other hand, from the turbulent kinetic energy $\bar{\omega}$ a convective velocity

$$u_c = \sqrt{\frac{2}{3}}\,\bar{\omega}^{1/2} \tag{21}$$

which is interpreted as the average speed of a convective element, can be defined. The basic idea is now that enthalpy cannot be carried with velocities exceeding u_c. Combining Eqs. 6, 20 and 21 we end up with the ratio between the enthalpy diffusion velocity and the speed of convective elements

$$\frac{u_D}{u_c} = -\frac{\sqrt{3/2}\,\alpha_s\,\Lambda\,T}{w}\,\frac{\partial s}{\partial r} \propto \frac{\partial \ln s}{\partial \ln r}\,, \tag{22}$$

that corresponds to a dimensionless entropy gradient with Λ as length-scale and w/T as entropy-scale. If $u_D/u_c > 1$, enthalpy is carried with velocities larger than u_c meaning that the diffusion approximation applicable only for small departures from equilibrium, is no longer valid. The major consequence of this violation is an overestimation of the convective enthalpy flux j_w.

In order to fix this problem the following limiting concept has been developed. The basic idea, that the enthalpy diffusion speed cannot exceed the velocity u_c of convective elements, suggests to limit u_D with u_c. Practically speaking we introduce this limit in the expression for Π (Eq. 6) obtaining a so-called "convective enthalpy flux limiter" in the form

$$\Pi = \frac{w}{T}\,u_c F_L\!\left[\frac{u_D}{u_c}\right] = \frac{w}{T}\,u_c F_L\!\left[-\sqrt{3/2}\;\alpha_s\,\frac{\Lambda\,T}{w}\,\frac{\partial s}{\partial r}\right]. \tag{23}$$

$F_L[x]$ denotes a function linear for $x < 1$, 1 for $x > 1$ and a smooth connection in between. Consequently for small values of u_D/u_c Eq. 23 limits to the original expression for Π whereas values larger than one lead to the free streaming value

$$\Pi = \frac{w}{T}\,u_c\,. \tag{24}$$

Concerning numerical radiation hydrodynamics it is important to remark that the connection between linear and constant part of F_L has to be smooth and differentiable for both F_L itself and its derivative requiring at least a polynom of $5^{\rm th}$ order. Test calculations of RR Lyrae pulsations with different versions for $F(x)$ (arcus tangens, hyperbolic tangens, polynomial connection) show that results do not depend on the particular choice of the limiter function.

In general the approximation of transport phenomena by diffusive processes is restricted to situations where the mean free path of the "particles" is much lower than the typical length scale of the problem. In that case the diffusion velocity is much lower than the corresponding particle velocity for the case of free streaming. A well known example is the radiation diffusion equation widely used in stellar structure, evolution and pulsation models (e.g. Alme & Wilson 1974 or Mihalas & Mihalas 1984). As long as the medium is optically thick meaning that a photon experiences a large number of collisions, the radiative flux in good approximation is given by a diffusion equation involving the temperature gradient. However, as soon as the optical depths become moderate to low the radiative flux is overestimated, which in the worst case causes photon velocities exceeding the speed of light. Similar to the above proposed enthalpy flux limiter the radiative flux has to be limited to the free streaming value, which is a well known concept in radiation theory since a long time (e.g. Mihalas & Mihalas, 1984). In Bono & Stellingwerf (1992) it is shown, that the inclusion of a radiative flux limiter only marginally affects the results of stellar pulsation models, indicating that in contrast to the convective diffusion approximation (cf. Sect. 4.3.2) radiation diffusion behaves well in stellar evolution and pulsation models.

In the following paragraphs we illustrate the outlined problem of too high diffusion velocities and their consequences by means of two completely different examples involving star formation and nonlinear stellar pulsation models.

4.3.1. Convection in protostellar collapse

The key flow-feature for testing the behaviour of a convection model in protostellar collapse flows is the accretion shock and its vicinity. This shock has Mach numbers starting at about 4 at the beginning of the main accretion phase and rises to 200 at the end of significant mass accretion. The physical situation is further complicated by the fact that due to the accretion process the envelope is thinned out and the accretion shock becomes optically thin and supercritical. We refer to Balluch (1991a,b,c) for a discussion of protostellar accretion flows. This regime is terra incognita for astrophysical convection models and represents a strong test for the physically plausible behaviour of a convection model in the extremely non-hydrostatic, nonlinear regime. The structure of a protostellar accretion shock for the collapse of a Jeans-critical solar mass isothermal cloud is discussed in Figs. 1 and 2. The flow in the vicinity of the accretion shock is shown for two cases: (1) original Kuhfuß model with the inclusion of radiative losses (Fig. 1) and (2) the modified model with radiative losses and enthalpy flux-limit (Fig. 2, cf. Sect. 4.3). Both are shown at an effective mass ($M_{\rm eff}$: $M(r)$ at $\tau_{\rm Ross} = 2/3$, $M_{\rm eff} = 0.033 M_\odot$, $L = 3.34 L_\odot$, $T_{\rm central} = 1.22\,10^4$ K, i.e. at the beginning of the main accretion phase. Turbulent pressure, overshooting and turbulent viscosity are neglected ($P_T = 0$, $\alpha_t = 0$, $\alpha_\mu = 0$). Fig. 2 (lower panel) shows temperature and Mach-number in the vicinity of the main accretion shock. Material falls almost freely from the right (larger radii) into the shock at $\mathrm{Mach} \approx -17$ and decelerates accross the shock to subsonic values and further to quasi-hydrostatic conditions downstream, i.e. below the shock. Material approaching the shock with temperatures of about 100 K is shock heated to a few 1000 K. Then it radiatively cools down in the radiative relaxation region. This produces the charactaristic temperature spike of a radiating shock wave. After radiative relaxation the temperature slowly rises over the scale height, H_p of the quasi-hydrostatic atmosphere ($H_p/r \approx 0.05$). Fig. 1 shows the behaviour of convection without the enthalpy flux limiter. The convective Mach-number u_c/c_s and the relative effective convective enthalpy diffusion velocity u_D/u_c are plotted. A non-zero convective Mach-number shows a convection zone and gives an indication about the strength of convection by comparing the convective velocity to the local isentropic sound speed. Nonconvective matter ($\mathrm{Mach}_{\rm conv} = 0$) advects into the shock and passes it without much net effect. Further in the hydrostatic part the outer part of the well developed mantle convective shell of the protostellar core is visible. The important point is the effective enthalpy diffusion velocity. The standard model, even with radiative losses produces an enthalpy flux that corresponds to an effective diffusion speed of more than 600 times the convective velocity. For the depicted convective Mach-numbers this is not only well beyond the validity of the diffusion approximation (above the free flow limit $j_w = \rho u_c w$) but also above the sound speed. This is unphysical for two reasons: (1) subsonic eddies cannot transfer energy at velocities exceeding the sound-speed and (2) no transfer process can exeed the free flow limit. The situation is completely analogous to respective limits in heat conduction and radiation diffusion. A main reason for using the moment equations of the radiation transfer equations instead of the radiation diffusion equation comes exactly from a similar radiation flux-feature in radiating shocks. To obtain a physically plausible convection description for the protostellar accretion shock we introduce the enthalpy flux-limiter as described in Sect. 4.3. Fig. 2 shows the structure of the accretion shock at the same effective mass as above. The effective enthalpy diffusion speed now remains bounded within $\pm u_c$ and a comparison with the convective Mach-number shows that convective enthalpy transfer also remains subsonic. We take this as the motivation to add the enthalpy flux-limiter to the standard model. Note that the shock is located at a smaller radius of $\approx 3.14\,10^{11}$ cm compared to $3.63\,10^{11}$ cm for the non-flux-limited convection model, an indication that the flux limiter also affects the global structure of the protostellar core.

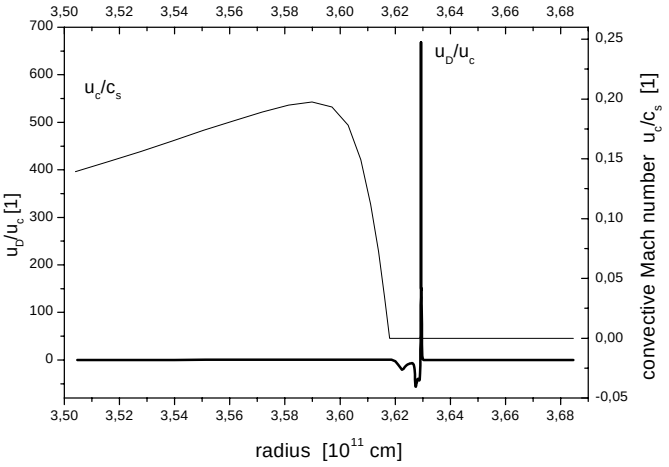

Fig. 1. Flow structure in the vicinity of a protostellar accretion shock without convective enthalpy flux-limiter. See text for details.

4.3.2. Convection in RR-Lyrae stars

As as second example we demonstrate the violation of the diffusion approximation for the case of pulsating RR Lyrae stars. In Fig. 3 we illustrate the situation for a typical hydrostatic RR Lyrae envelope near the red edge of the instability strip. The model is calculated by a direct forward integration of the stellar structure equations including the Kuhfuß convection model without turbulent pressure and overshooting. The convective structure with respect to the temperature is depicted by means of the convective Mach number u_c/c_s (thick line, c_s denoting the speed of sound) and the radiative luminosity (thin line) in the lower panel. The thermodynamic situation can be inferred from the run of ∇_s in the upper panel (thin line). The labels at the minima refer to the ionisation zones of hydrogen and helium which are essential for the pulsational driving. As a consequence of the minima in ∇_s meaning that a compression of the gas leads to excitation of internal degrees of freedom rather than to an increase of the temperature, each ionisation zone is accompanied by a convection zone indicated by the minima of the radiative

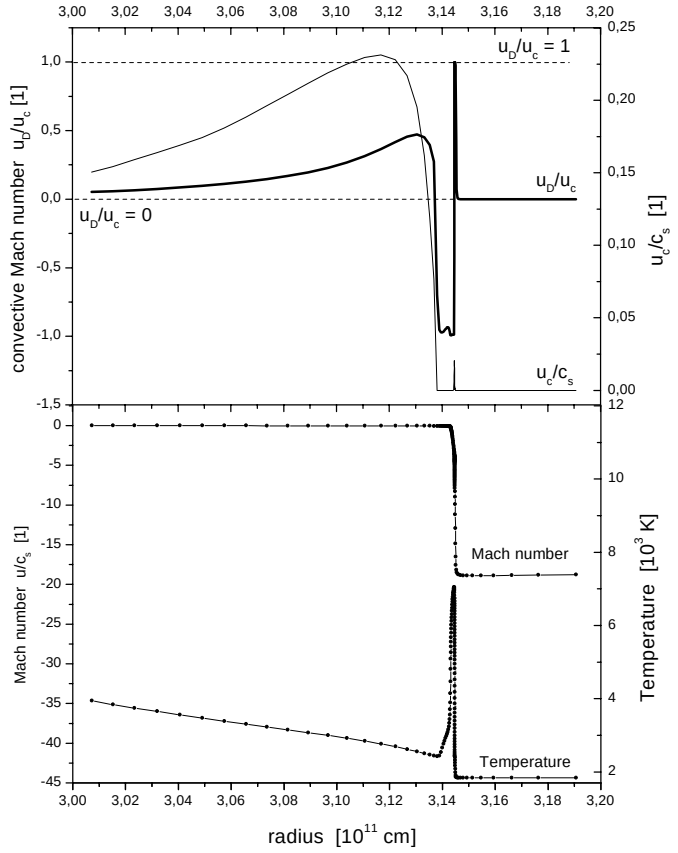

Fig. 2. Flow structure in the vicinity of a protostellar accretion shock with convective enthalpy flux-limiter. Each point in the lower panel corresponds to one cell in the numerical computation. See text for details.

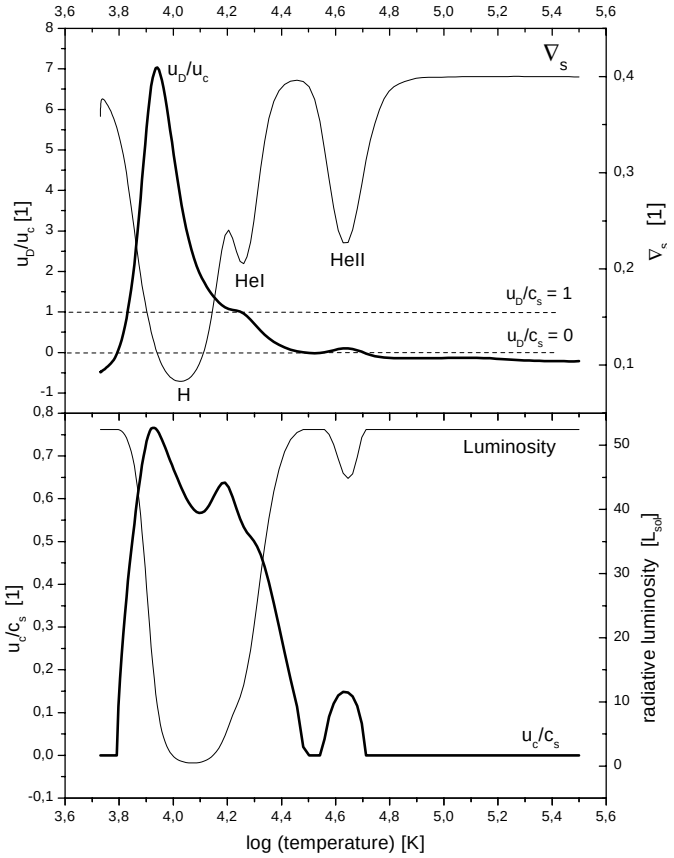

Fig. 3. Convective structure for an RR Lyrae envelope with stellar parameters of $M = 0.65\mathrm{M}_\odot$, $\log(L/\mathrm{L}_\odot) = 1.72$, $T_{\rm eff} = 6400$ K and XYZ=(0.760, 0.239, 0.001). We use OPAL opacities and the equation of state from Wuchterl (1990). The outer boundary is located on the left-hand side while the right-hand side corresponds to some point in the interior of the model. See text for details.

lumimosity and the corresponding maxima of the convective Mach number.

The violation of the diffusion approximation can be observed from the run of u_D/u_c (thick line in the upper panel). Starting at the interior (right side) u_D/u_c remains lower than zero (indicating convective stability) down to the point where HeII starts recombination. In the subsequent HeII convection zone u_D/u_c increases only slightly above zero and becomes again lower than zero when HeII is fully recombined. Proceeding to even lower temperatures the situation alters substantially in the combined H-HeI ionisation zone. u_D/u_c reaches 1 when HeI recombines, peaks at 7.3 in the center of the hydrogen ionisation zone and finally decreases to values lower than zero when hydrogen recombination is terminated. Consequently in the regions with $u_D/u_c > 1$ the diffusion approximation is invalid yielding too high convective enthalpy fluxes.

The effect of limiting the enthalpy diffusion velocity and henceforth the convective enthalpy flux is illustrated in Fig. 4. First, we observe that the HeII convection zone lying within the linear part of F_L remains almost unaffected. The picture changes considerably for the combined H-HeI zone where the effect of limiting u_D with u_c can be seen in the convective Mach number (lower panel, thick line) and in the radiative luminosity (thin line) as well. The thickness of the convection zone decreases substantially leading to a decrease of the energy carried by convection.

It is important to note that in the case of pulsating stars the violation of the diffusion approximation is illustrated by means of the hydrostatic stellar structure of a typical pulsating star, which represents only the mean background structure around which the star oscillates. Even though the nonlinearity of classical stellar pulsations is weak leading only to small perturbations from the equilibrium we expect temporal variations of u_D/u_c during the pulsation cycle. In that sense a more detailed investigation of the enthalpy diffusion limit would require a description of the full time-dependent behavior over one pulsation period. We refer to a companion paper (Feuchtinger 1998b) dealing in particular with convection in pulsating stars for further discussion.

Nevertheless, in order to provide a feeling for the influence of the enthalpy flux limiter in Fig. 5 (upper panel) we compare the corresponding nonlinear full amplitude light curves computed with the standard diffusion formulation (thin line) and the enthalpy flux limit (thick line). For easier orientation a typical observed RR Lyrae light curve obeying a similar pul-

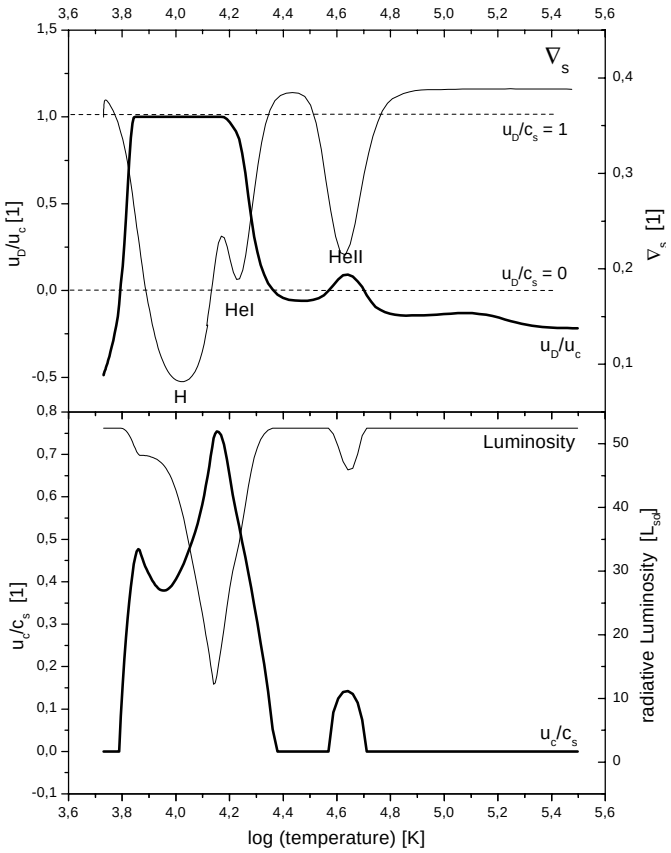

Fig. 4. Same as Fig. 3 but calculated with limited enthalpy diffusion velocity (see text for details).

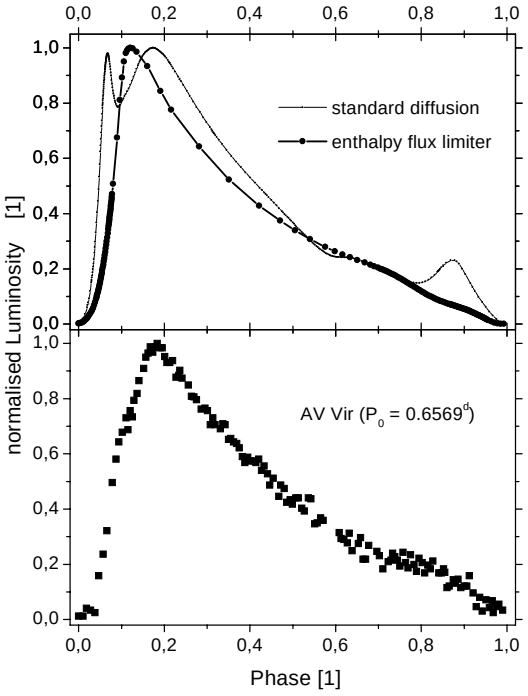

Fig. 5. *Upper panel:* Nonlinear full amplitude RR Lyrae light curve using the standard diffusion formulation (thin line) and the enthalpy flux limiter (thick line, each dot corresponds to one time step of the numerical computation). *Lower panel:* Typical observed RR Lyrae (RRab) light curve (from Lub, 1977). In order to provide a detailed comparison of the shapes the light curves are scaled to the same normalised amplitude. Fundamental periods and amplitudes of the theoretical models correspond to 0.648 days and 0.92 mag in the case of standard diffusion and to 0.651 days and 1.15 mag in case of the flux limited diffusion, respectively.

sation period is depicted in the lower panel. The light curves are computed with our adaptive radiation hydrodynamics code (Feuchtinger & Dorfi 1994) including the Kuhfuß convection model.

Without going into too much details we emphasise the differences of the light curves demonstrating the influence of the flux limiter on their shape and in particular the appearance of a spike before maximum light in absence of the enthalpy diffusion limit. As far as we explored the space of the free convective parameters of the original Kuhfußmodel (cf. Sect. 7) no meaningful combination leads to a significant decrease of the spike.

Even though observations indicate secondary features like small bumps before the maximum in some RR Lyrae stars (Bono & Stellingwerf 1984, Lub 1977), spikes like the depicted one showing nearly the same amplitude than the maximum itself are not visible in observed RR Lyrae light curves. If we further proceed to models near the red boundary of the instability strip characterised by low effective temperatures and increasing influence of turbulent convection, the spike becomes more and more the dominant feature in the light curve. Additionally the appearance of this spike is accompanied by a significant rise of the low order Fourier phases achieved by a detailed analysis of the light curves which is in disagreement with observations (Simon 1985, Feuchtinger & Dorfi 1997). A thorough analysis of the influence of limiting the enthalpy flux on the results of nonlinear pulsation calculations will be presented in a companion paper which currently is under development (Feuchtinger 1998b).

It is interesting to note that similar spikes near maximum light also apear in the nonlinear convective RR Lyrae models of Bono et al. (1997) using the convection model of Stellingwerf (1982) which in several aspects is similar to the original Kuhfuß model.

5. The complete convection model

The complete time-dependent one-equation model of turbulent convection including the modifications presented in Sect. 4 is summarised in Table 1. For particular astrophysical applications like nonlinear stellar pulsations or protostellar collapse calculations the turbulent kinetic energy equation has to be solved together with the equations of radiation hydrodynamics (e.g. Dorfi & Feuchtinger 1995). In this context all necessary reformulations and adaptions are discussed in detail in Wuchterl (1995a). The last two lines in Table 1 correspond to terms providing the coupling to the radiation hydrodynamics. The convective enthalpy flux j_w enters as an additional source term in the energy equation ($\nabla \cdot j_w$), and the viscous momentum and energy gener-

Table 1. Summary of the complete time-dependent one-equation model of turbulent convection originally developed by Kuhfuß (1986). Refer to Table A1 for a comprehensive list of symbols.

equation / physical quantity	name
$\frac{d\bar{\omega}}{dt} = S_{\bar{\omega}} - \tilde{S}_{\bar{\omega}} - D_{\rm rad} - \frac{1}{\rho}\nabla\cdot j_t - \frac{P_t}{\rho}\nabla\cdot u + \frac{1}{\rho}E_Q$	turbulent kinetic energy equation
$S_{\bar{\omega}} = \frac{T}{P}\nabla_s\frac{\partial P}{\partial r}\Pi$	turbulent driving through bouyancy forces
$\Pi = \sqrt{\frac{2}{3}}\frac{w}{T}\bar{\omega}^{1/2}F_L\left[-\sqrt{\frac{3}{2}}\frac{\alpha_s\Lambda T}{w}\frac{\partial s}{\partial r}\right]$	correlation between velocity and entropy fluctuations
$\frac{\partial s}{\partial r} = \frac{1}{T}\frac{\partial e}{\partial r} - \frac{P}{\rho^2 T}\frac{\partial\rho}{\partial r} = -\frac{c_P}{H_{\rm p}}(\nabla - \nabla_s)$	specific entropy gradient
$\tilde{S}_{\bar{\omega}} = c_D\frac{\bar{\omega}^{3/2}}{\Lambda}$	turbulent dissipation
$D_{\rm rad} = \frac{\bar{\omega}}{\tau_{\rm rad}}$	radiative cooling of convective elements
$\tau_{\rm rad} = \frac{c_p\kappa\rho^2\Lambda^2}{4\sigma T^3\gamma_{\rm R}^2}$	radiative cooling time scale of convective elements
$j_t = \alpha_t\rho\Lambda\bar{\omega}^{1/2}\frac{\partial\bar{\omega}}{\partial r}$	turbulent kinetic energy flux
$P_t = \frac{2}{3}\rho\bar{\omega}$	turbulent pressure
$E_Q = \frac{4}{3}\mu_Q\left\{\frac{\partial u}{\partial r} - \frac{u}{r}\right\}^2$	turbulent viscous energy dissipation
$\mu_Q = \alpha_\mu\rho\Lambda\bar{\omega}^{1/2}$	turbulent viscosity
$\frac{1}{\Lambda} = \frac{1}{\alpha_{\rm ML}H_P^{\rm stat}} + \frac{1}{\beta_r r}$	mixing length
$H_P^{\rm stat} = \frac{r^2 P}{G m_r\rho}$	hydrostatic pressure scale hight
$j_w = \rho T\Pi$	convective enthalpy flux entering the energy equation
$U_Q = \frac{1}{r^3}\frac{\partial}{\partial r}\left\{\frac{4}{3}\mu_Q r^3\left[\frac{\partial u}{\partial r} - \frac{u}{r}\right]\right\}$	turbulent viscous momentum generation entering the equation of motion

ation U_Q and E_Q have to be added to the righthand side of the equation of motion and the energy equation, respectively.

6. Local static solution

In Kuhfuß (1987) it is shown, that except for the radiative cooling the local static solution of the original model corresponds to the MLT if the free parameters α_s and c_D are chosen in the following way:

$$\alpha_s = \frac{1}{2}\sqrt{\frac{2}{3}} \tag{25}$$

$$c_D = \frac{8}{3}\sqrt{\frac{2}{3}} \tag{26}$$

Correspondingly we derive the local static solution for the extended model presented in the preceding paragraph. By assuming the time derivative and the gas velocity u in Eq. 4 to vanish and neglecting overshooting ($\alpha_t = 0$ the equation for the turbulent kinetic energy $\bar{\omega}$ reads

$$\frac{T}{P}\frac{\partial P}{\partial r}\nabla_s\Pi - c_D\frac{\bar{\omega}^{3/2}}{\Lambda} - \frac{\bar{\omega}}{\tau_{\rm rad}} = 0 \tag{27}$$

Using for the first the original diffusion approximation for Π (Eq. 6) and assuming convective instability ($\partial s/\partial r < 0$) Eq. 27 represents a quadratic equation for u_c with the solution.

$$u_c = \sqrt{\frac{1}{6}}\frac{\Lambda}{c_D} \times\left\{\left[\frac{1}{\tau_{\rm rad}^2} + 4c_D\alpha_s\frac{T}{P}\frac{\partial P}{\partial r}\nabla_s\frac{\partial s}{\partial r}\right]^{1/2} - \frac{1}{\tau_{\rm rad}}\right\} \tag{28}$$

Following Kuhfuß (1987) we introduce u_c into the total energy ballance for a hydrostatic configuration given by

$$j_w + F_{\rm rad} = \frac{L}{4\pi r^2} \tag{29}$$

with L denoting the total luminosity. By employing the usual radiation diffusion equation

$$F_{\rm rad} = \frac{k_{\rm rad}T}{H_P}\nabla, \qquad \text{with} \qquad k_{\rm rad} = \frac{16\sigma T^3}{3\kappa\rho}$$

for the radiative energy flux $F_{\rm rad}$ and introducing the radiative temperature gradient

$$\nabla_{\rm rad} = \frac{H_P}{k_{\rm rad}T}\frac{L}{4\pi r^2}, \tag{30}$$

from Eq. 29 we get

$$\sqrt{3/2}\,\alpha_s\,\Lambda\,u_c\,\frac{c_P}{H_P}\,(\nabla-\nabla_s)=(\nabla_{\rm rad}-\nabla)\,, \tag{31}$$

which represents a nonlinear equation for the actual temperature gradient ∇. Using now the above expression for u_c and the dimensionless variables

$$f\;=\;\frac{\nabla-\nabla_s}{\nabla_{\rm rad}-\nabla_s}\qquad\text{and} \tag{32}$$

$$x\;=\;\frac{U}{\sqrt{\nabla_{\rm rad}-\nabla_s}} \tag{33}$$

with U defined as

$$U=\frac{9k_{\rm rad}}{\alpha_{\rm ML}^2\,\rho\,H_P}\,(2\nabla_s c_P^3 T)^{-1/2} \tag{34}$$

we end up with the cubic equation

$$\frac{9}{8}\frac{\alpha_s}{c_D}\frac{f}{x}\left\{\left[\left(\frac{\gamma_R^2}{12}\right)^2 x^2+2\alpha_s\,c_D f\right]^{1/2}-\frac{\gamma_R^2}{12}\,x\right\} =1-f \tag{35}$$

for ∇, which can be expressed as

$$\nabla=f\,\nabla_{\rm rad}+(1-f)\,\nabla_s\,. \tag{36}$$

The above cubic equation is similar to the corresponding one of the MLT which in f and x reads as

$$\frac{9}{8x}\,\left\{(x^2+f)^{1/2}-x\right\}^3=1-f\,. \tag{37}$$

In Fig. 6a we plot the solution $f(x)$ of Eq. 35 for two values of $\gamma_{\rm R}$ (dotted and dashed line) in comparison with the MLT (solid thick line) and the standard Kuhfuß solution (solid thin line). In order to illustrate the physical meaning of the dimensionless variable x the spatial run of x for a static solar and a typical static RR Lyrae model are shown in Fig. 6c. In the optically thick interior x remains much less than one, while x becomes significantly greater than one in the outer optically thin region (at lower temperatures). As can be inferred from Fig. 6b, significant deviations from the MLT occur in the region between $x=10^{-3}$ and $x=10^2$ (shaded area in panel c) and depend on the choice of the free parameter $\gamma_{\rm R}$. In case of the standard value of $\gamma_{\rm R}=2\sqrt{3}$ given for the 3-equation model in Kuhfuß (1987) the maximum deviation is about 30% at $x\sim 0.7$. If $\gamma_{\rm R}$ is set to $8\sqrt{3}$ the deviation is minimised at about 7%. A comparison to the standard Kuhfuß formulation yields the deviation from the MLT to be considerably reduced by the additional term accounting for radiative losses in particular in the region of $x>1$.

Using Eq. 23 instead of the original expression for Π the solution of Eq. 27 clearly deviates form the MLT solution (cf. Sect. 8) Consequently the cubic equation is substituted by a nonlinear algebraic equation for the actual temperature gradient.

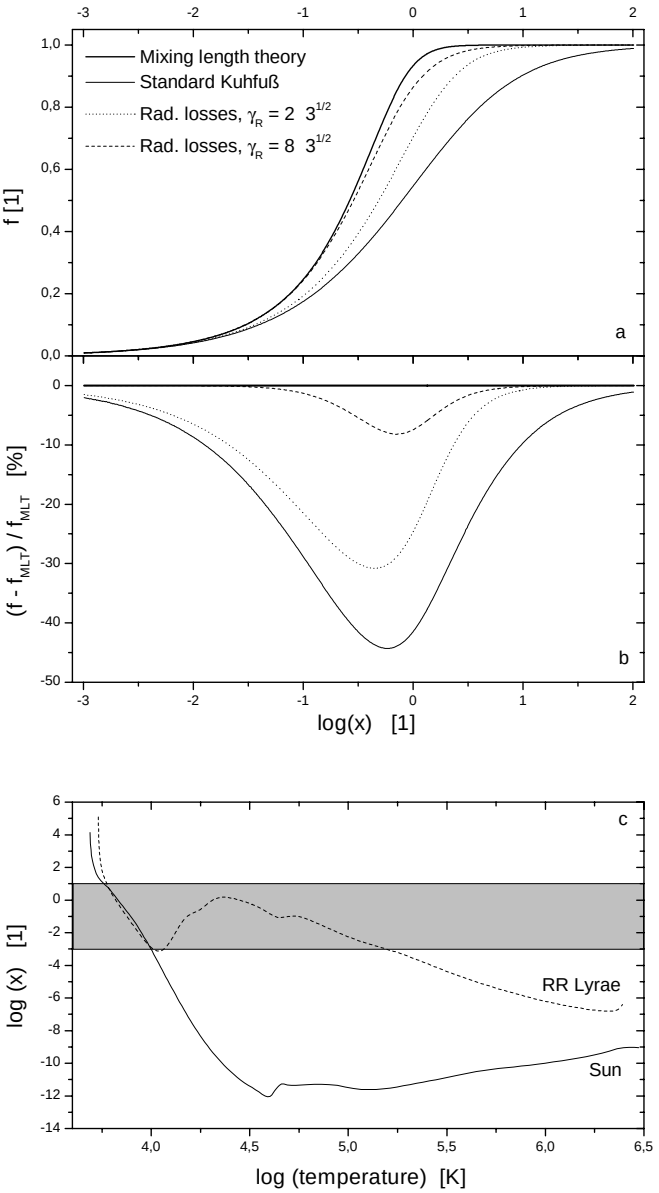

Fig. 6a–c. Solution of the cubic equation for the Kuhfuß standard model and the model including radiative losses in comparison with the mixing length theory **a**. The relative deviations to the MLT are shown in panel **b**. Note that $\nabla=f\,\nabla_{\rm rad}+(1-f)\,\nabla_s$. Panel c depicts the spatial run of the dimensionless quantity x depending only on the background structure for the solar envelope (solid line) and for a typical RR Lyrae envelope (dashed line). The shaded area corresponds to the range of x plotted in panel **a** and **b**.

7. Free parameters

Bearing in mind the lack of a self-consistent convection theory every model of turbulent convection has to deal with several free parameters. Depending on the type of astrophysical applications these parameters have to be choosen in accordance to reproduce the corresponding observational results. Concerning the modified Kuhfuß-model presented in this paper each source and sink term in the turbulent kinetic energy equation involves essentially one free parameter. A summary of all parameters is given in Table 2. As already shown in Sect. 6 the correspondence of the local static solution to the mixing length theory leads to standard values for α_s and c_D. The value for γ_R is chosen in

Table 2. Free parameters and standard values of the modified Kuhfuß-model for time-dependent turbulent convection.

parameter	standard value	physical meaning
$\alpha_{\rm ML}$	1.5	mixing length
α_s	$\frac{1}{2}\sqrt{\frac{2}{3}}$	turbulent driving
c_D	$\frac{8}{3}\sqrt{\frac{2}{3}}$	turbulent dissipation
$\gamma_{\rm R}$	$2\sqrt{3}$	radiative cooling
α_μ	–	turbulent viscosity
α_t	$0.6093\,\alpha_s$	overshooting distance
β_r	0.1	weak gravity mixing length

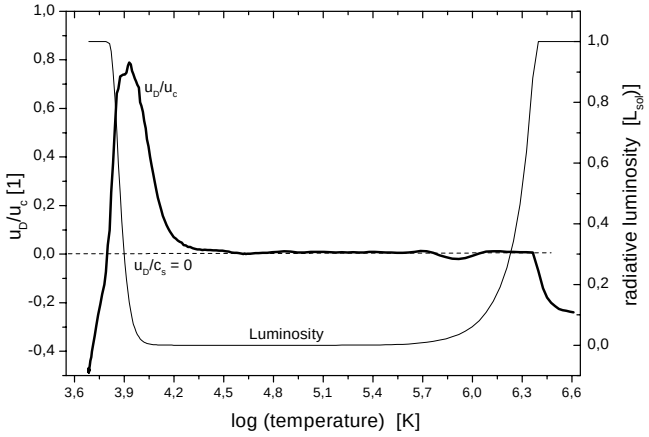

Fig. 7. Convective solar envelope using the modified Kuhfuß convection model presented in this article.

accordance to the 3-equation model of Kuhfuß (1987) where the same radiative time scale is used to model the radiative losses. Although it seems preferable to use this MLT limit representing a standard reference point we emphasize that this choice is not mandatory. The standard value for the overshooting parameter α_t is estimated in Kuhfuß (1987) and the value for β_r is a typical value used in protoplanetary models.

8. Comparison with the solar standard model

Accurate helioseismological observations in combination with so-called solar standard models provide a detailed picture of the solar convection zone. In particular several physical quantities at the bottom of the convection zone like radius, temperature and speed of sound can be derived (e.g. Ciacio et al. 1997). Usually adopting the MLT, clearly the properties of these models depend on the employed model for turbulent convection. In Sect. 6 we demonstrate that the local static limit of the modified Kuhfuß-model approximates the MLT structure, if the enthalpy flux limiter is omitted. On the other hand, the inclusion of the enthalpy flux limiter causes a deviation from the MLT-limit and consequently it is interesting to investigate this influence on the structure of the solar convection zone. Therefore we compute a solar-like envelope by integrating the stellar structure equations both with and without the enthalpy flux limiter. For the stellar parameters we adopt $L = 3.844{\cdot}10^{33}{\rm erg/s}$ and $R = 6.96{\cdot}10^{10}{\rm cm}$ (Ciacio et al. 1997) yielding an effective temperature of 5777.1 K. The results of the comparison between MLT and flux limiter version are summarised in Table 3 listing the values for radius and temperature at the bottom of the convection zone. Additionally we include the corresponding values for a recent solar standard model published in Ciacio et al. (1997) and the values for the original Kuhfuß model without radiative cooling and enthalpy flux limiter. Bearing in mind that by performing a simple forward integration of the stellar structure equations we only consider the envelope (i.e. we have to prescribe the luminosity) we first note that our calculated parameters are in reasonable agreement with the standard model data. The main conclusion from Table 3 is, that practically speaking the enthalpy flux limiter has no influence on the convective structure of solar-like models, which easily can be explained by viewing Fig. 7. From the run of u_D/u_c (thick line) it becomes evident that within the whole convection zone (indicated by the deep depression of the radiative luminosity, thin line) the enthalpy diffusion speed always remains lower than the speed of the convective elements causing no violation of the diffusion approximation in Eq. 6. The physical background for this behavior can be inferred from rewriting u_D/u_c with the help of Eq. 7,

$$\frac{u_D}{u_c} = \sqrt{3/2}\,\alpha_s\,\alpha_{\rm ML}\,\frac{c_P\,T}{w}\,(\nabla - \nabla_s) \tag{38}$$

In fact u_D/u_c essentially is proportional to $\nabla - \nabla_s$ meaning that the diffusion approximation is valid as long as the superadiabaticity of the actual temperature gradient remains small. We illustrate this in Figs. 8 and 9 depicting the spatial run of the actual temperature gradient (∇) for the RR Lyrae model discussed in Sect. 4.3.2 and the solar-like model, respectively. The two limits for the actual gradient ∇ (thick dots) are the isentropic gradient ∇_s (thin solid line) established at maximum convective efficiency and the radiative gradient $\nabla_{\rm rad}$ (thin dashed line), which applies if the whole energy is carried by radiation. Evidently in the solar-like case the temperature gradient stays practically isentropic throughout almost the whole convection zone, becoming superadiabatic only in the outermost part of the hydrogen ionisation zone. Correspondingly u_D/u_c remains small meaning that the flux limited gradient equals to the non-limited one. On the contrarry the temperature gradient in the RR Lyrae envelope is highly superadiabatic causing the high values of u_D/u_c (Fig. 3) as already discussed in Sect. 4.3.2. Summarising the above discussion the proposed enthalpy flux limit becomes important whenever convection causes highly superadiabatic temperature gradients as the case e.g. in envelopes of classical pulsating stars like RR Lyrae's and Cepheids.

The last line in Table 3 refers to the solar model computed with the original Kuhfuß model. A comparison with the first line yields considerable differences caused by the missing of radiative cooling.

Table 3. Radius (R_b) and temperature (T_b) at the bottom of the convection zone for the solar like model with and without enthalpy flux limiter (see text for details).

model	$R_b/\mathrm{R}_\odot$ [1]	T_b [K]
standard diffusion	0.7167	2.1781
enthalpy flux limit	0.7165	2.1796
Ciacio et al. (1997)	0.7160	2.1700
original Kuhfuß (1987)	0.7019	2.3325

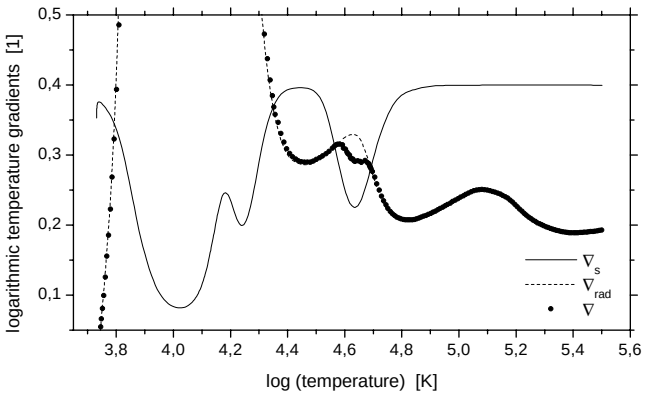

Fig. 8. Radiative, isentropic and actual temperature gradient for the RR Lyrae model of Fig. 4 (values above 0.5 are clipped, see text for details

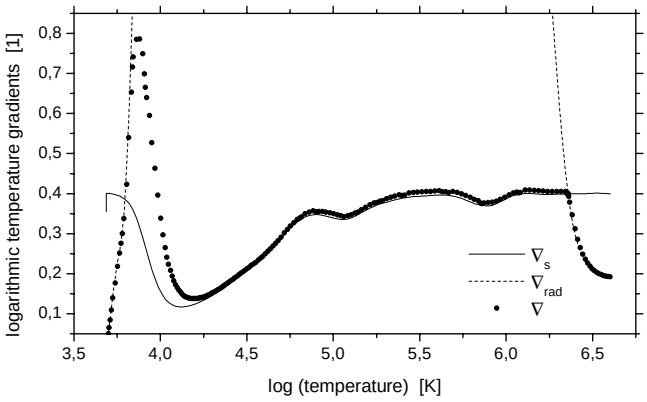

Fig. 9. Radiative, isentropic and actual temperature gradient for the solar model model of Fig. 4 (values above 0.8 are clipped, see text for details.

9. Concluding remarks

We have given a convection model that, together with the equations of radiation hydrodynamics constitutes for a time-dependent set of equations that for the first time contains the classical stellar structure equations, with a close approximation to mixing length convection as a limit for hydrostatic equilibrium and vanishing motion and that is also capable of describing the approach to reach that limit along an evolutionary path. The latter point is essential for dynamical star and planet formation calculations and is satiesfied because the Kuhfuß model is capable of describing the onset of convection starting from a stable stratification without any assumptions about a seed-turbulence. Moreover our modified Kuhfuß convection model agrees with MLT superadiabaticity to better than 7% in the local static and non- fluxlimited case.

We have demonstrated that the convection model correctly describes the Sun and RR-Lyrae pulsations and behaves physically plausible in protostellar collapse flows, even in the case of interaction with supercritical accretion shocks. Detailed results of those computations will be presented in consecutive papers (e.g. Feuchtinger 1998a,b).

Finally the article can be summarised by saying that we have successfully integrated two rules, well known in classical stellar structure theory, into convective radiation hydrodynamics: (1) that radiative losses of convective eddies cannot be neglegted at moderate optical depths, and (2) that convective velocities have to be truncated at the sound-speed.

Acknowledgements. This work is supported by the *Fonds zur Förderung der wissenschaftlichen Forschung (FWF)* under project numbers S7305–AST and S7307–AST.

Appendix A: list of symbols

A comprehensive list of symbols is given in Table A1

Table A1. List of symbols

Gas dynamics		
r	cm	radius
t	s	time
m_r	g	mass within radius r
ρ	$\mathrm{g\,cm^{-3}}$	density
e	$\mathrm{erg\,g^{-1}}$	specific internal energy
P	$\mathrm{dyn\,cm^{-2}}$	pressure
T	K	temperature
u	$\mathrm{cm\,s^{-1}}$	velocity
s	$\mathrm{erg\,g^{-1}\,K^{-1}}$	specific entropy
w	$\mathrm{erg\,g^{-1}}$	specific enthalpy
H_P	cm	pressure scale hight
∇	1	actual temperature gradient
∇_{rad}	1	radiative temperature gradient
L	$\mathrm{erg\,s^{-1}}$	total luminosity
F_{rad}	$\mathrm{erg\,cm^{-2}\,s^{-1}}$	radiative flux
Constitutive relations and physical constants		
c_s	$\mathrm{cm\,s^{-1}}$	speed of sound
∇_s	1	isentropic temperature gradient
c_P	$\mathrm{erg\,g^{-1}\,K^{-1}}$	secific heat at constant pressure
κ	$\mathrm{cm\,g^{-1}}$	opacity
G	$\mathrm{cm^3\,g^{-1}\,s^2}$	gavitational constant
σ	$\mathrm{erg\,cm^{-2}\,K^{-4}}$	Stefan-Boltzmann constant
Turbulent convection		
$\bar{\omega}$	$\mathrm{erg\,g^{-1}}$	specific turbulent kinetic energy
Λ	cm	mixing length
u_c	$\mathrm{cm\,s^{-1}}$	convective velocity
$S_{\bar{\omega}}$	$\mathrm{erg\,g^{-1}\,s^{-1}}$	turbulent driving function
$\tilde{S}_{\bar{\omega}}$	$\mathrm{erg\,g^{-1}\,s^{-1}}$	turbulent dissipation function

Table A1. (continued)

Π	$\mathrm{cm^3\,s^{-3}\,K^{-1}}$	velocity-entropy correlation
D_{rad}	$\mathrm{erg\,g^{-1}\,s^{-1}}$	radiative cooling
τ_{rad}	s	radiative cooling time scale
j_w	$\mathrm{erg\,cm^{-2}\,s^{-1}}$	convective enthalpy flux
j_t	$\mathrm{erg\,cm^{-2}\,s^{-1}}$	turbulent kinetic energy flux
P_t	$\mathrm{dyn\,cm^{-2}}$	turbulent pressure
μ_Q	$\mathrm{cm^2\,s^{-1}}$	turbulent viscosity
E_Q	$\mathrm{erg\,cm^{-3}\,s^{-1}}$	turbulent viscous energy generation
U_Q	$\mathrm{g\,cm^{-2}\,s^{-2}}$	turbulent viscous momentum generation

References

Alme M.L., Wilson J.R., 1974, ApJ 194, 147

Baker N., 1987, In: Meyer-Hofmeister E., Thomas H.C., Hillebrandt W. (eds.) Physical Processes in Comets, Stars and Active Galaxies. Springer, Berlin, p. 105

Balluch M., 1991a, A&A 243, 168

Balluch M., 1991b, A&A 243, 187

Balluch M., 1991c, A&A 243, 205

Bono G., Stellingwerf R.F., 1992, Mem. Soc. Astron. It. 63, 357

Bono G., Stellingwerf R.F., 1994, ApJS 93, 233

Bono G., Caputo F., Castellani V., Marconi M., 1997, A&AS 121, 327

Canuto V., Mazzitelli I., 1991, ApJ 370, 295

Ciacio F., Degl'Innocenti S., Ricci B., 1997, A&AS 123, 449

Deupree R.G., 1984, ApJ 282, 274

Deupree R.G., 1986, ApJ 303, 649

Dorfi E.A., Drury L.O'C., 1987, J. Comp. Phys. 69, 175

Dorfi E.A., Feuchtinger M.U., 1995, Comp. Phys. Comm. 89, 69

Feuchtinger M.U., 1998a, A&A 337, L31

Feuchtinger, M.U., 1998b, in prep.

Feuchtinger M.U., Dorfi, E.A., 1994, A&A 291, 225

Feuchtinger M.U., Dorfi E.A., 1997, In: Guzik J.A. (ed.) A half century of stellar pulsations. ASP Conference Series, Los Alamos

Glasner S.A., Livne E., 1995, ApJ 445, L149

Kippenhahn R., Weigert A., 1990, Stellar Structure and Evolution. Springer, Berlin, p. 42

Kuhfuß R., 1986, A&A 160, 116

Kuhfuß R., 1987, Ein Modell für zeitabhängige Konvektion in Sternen. PhD-Thesis, TU München

Lub, J., 1977, A&AS 29, 345

Mihalas D., Mihalas B.W., 1984, Foundatios of Radiation Hydrodynamics. Oxford University Press, New York

Simon N.R., 1985, ApJ 299, 723

Starrfield S., Cox A.N., 1989, In: White dwarfs. Proceedings of IAU Coll. 114, Springer, Berlin, p. 115

Stellingwerf R.F., 1982, ApJ 262, 330

Wuchterl G., 1990, A&A 238, 83

Wuchterl G., 1995a, Comp. Phys. Comm. 89, 119

Wuchterl G., 1995b, Earth, Moon and Planets 67, 51